JES

JOURNAL OF ENVIRONMENTAL SCIENCES

ISSN 1001-0742
CN 11-2629/X

March 1, 2013 Volume 25 Number 3
www.jesc.ac.cn

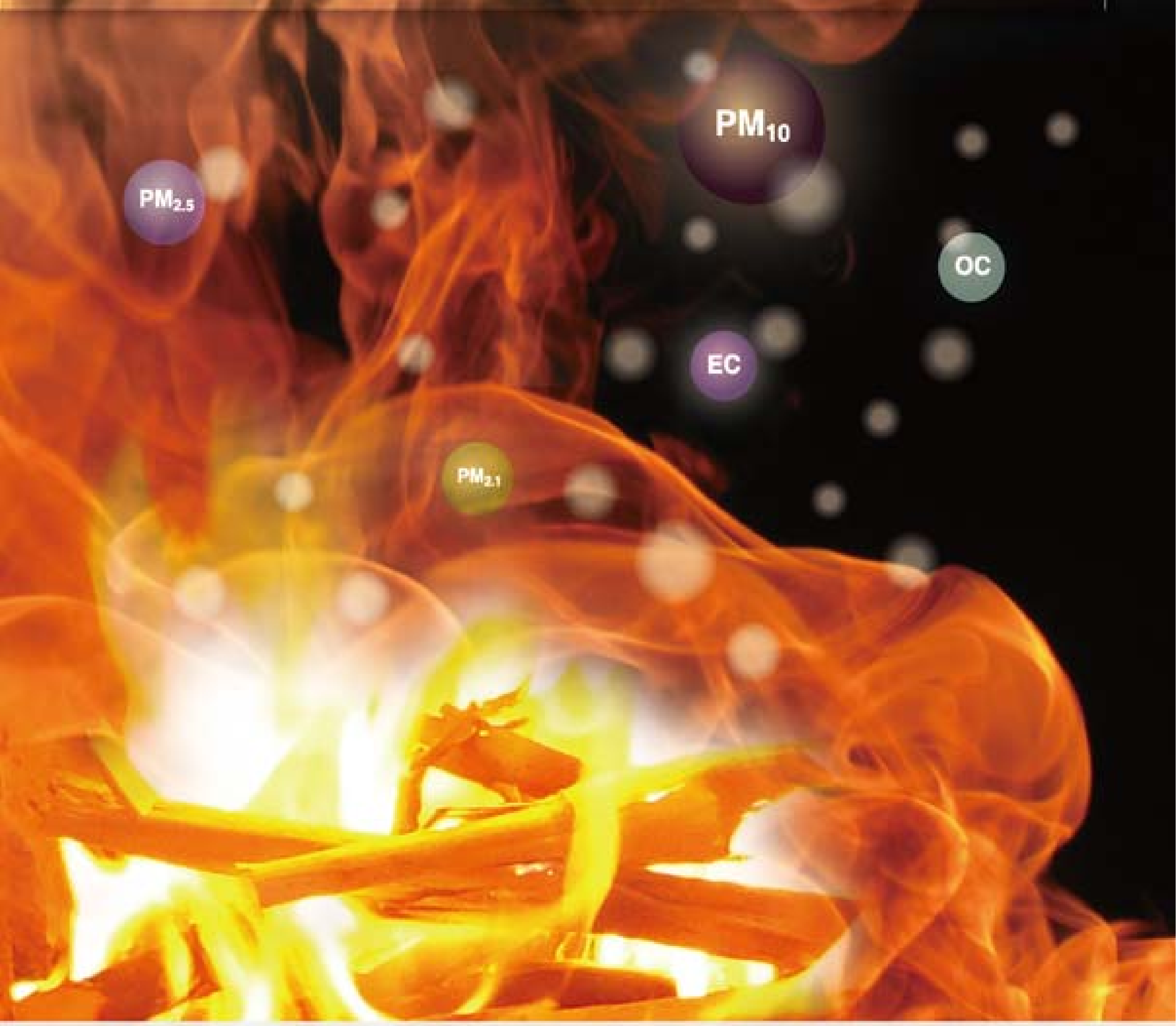

ELSEVIER
Science Press

Sponsored by
Research Center for Eco-Environmental Sciences
Chinese Academy of Sciences

ISSN 1001–0742 **Journal of Environmental Sciences** Vol. 25 No. 3 2013

CONTENTS

Serial parameter: CN 11-2629/X*1989*m*218*en*P*25*2013-3

Available online at www.sciencedirect.com

ScienceDirect

Journal of Environmental Sciences 2013, 25(3) 537–546

JOURNAL OF ENVIRONMENTAL SCIENCES
ISSN 1001-0742
CN 11-2629/X
www.jesc.ac.cn

Emission inventory evaluation using observations of regional atmospheric background stations of China

Xingqin An[1,*], Zhaobin Sun[2], Weili Lin[1], Min Jin[1], Nan Li[1]

1. Chinese Academy of Meteorological Sciences, China Meteorological Administration, Beijing 100081, China. E-mail: anxq@cams.cma.gov.cn
2. Beijing Meteorological Observatory, Beijing 100089, China

Received 18 June 2012; revised 22 August 2012; accepted 31 August 2012

Abstract

Any accurate simulation of regional air quality by numerical models entails accurate and up-to-date emissions data for that region. The INTEX-B2006 (I06), one of the newest emission inventories recently popularly used in China and East Asia, has been assessed using the Community Multiscale Air Quality model and observations from regional atmospheric background stations of China. Comparisons of the model results with the observations for the species SO_2, NO_2, O_3 and CO from the three regional atmospheric background stations of Shangdianzi, Longfengshan and Linan show that the model can basically capture the temporal characteristics of observations such as the monthly, seasonal and diurnal variance trends. Compared to the other three species, the simulated CO values were grossly underestimated by about two-third or one-half of the observed values, related to the uncertainty in CO emissions. Compared to the other two stations, Shangdianzi had poorer simulations, especially for SO_2 and CO, which partly resulted from the site location close to local emission sources from the Beijing area; and the regional inventory used was not capable of capturing the influencing factors of strong regional sources on stations. Generally, the fact that summer gave poor simulation, especially for SO_2 and O_3, might partly relate to poor simulations of meteorological fields such as temperature and wind.

Key words: evaluation; CMAQ model; INTEX-B2006 inventory; regional atmospheric background stations

DOI: 10.1016/S1001-0742(12)60082-5

Introduction

Emission inventory and meteorological parameters are the two key inputs for air quality models. Accurate simulation and forecast of regional air quality by numerical models requires accurate and up-to-date emission data for that region. Also, emission inventories play an important role in understanding air pollution and guiding emissions control policy (Jiang and Tang, 2002). Numerous studies have indicated that one of the major uncertainties involved in air quality models arises from deficiencies in emission inventories (Hanna et al., 1998; Bergin et al., 1999; Placet et al., 2000).

In the past 20 years, some emission inventories have been compiled for China that include one species, such as carbonaceous aerosol emissions (Streets et al., 2001; Bond et al., 2004; Cao et al., 2006), or several primary species, such as SO_2, NOx, CO_2, CO, CH_4, NMVOC, BC, OC, and NH_3 (Streets et al., 2003a). These inventories consist of China's gaseous or aerosol emissions at the national level or part of regional emission inventories. The Transport and Chemical Evolution over the Pacific (TRACE-P) emission inventory (Streets et al., 2003a) is a bottom-up emission inventory of the fuel consumption information and emission factors for Asian countries, which was constructed for the TRACE-P experiment (Transport and Chemical Evolution over the Pacific) under the auspices of the National Aeronautics and Space Administration (Jacob et al., 2003; Streets et al., 2003a, 2003b). Since the TRACE-P emission inventory was released, it has become the most popular inventory used in regional chemical transport models in the past several years, and some evaluation work on TRACE-P emission inventories has also been carried out using regional models and chemical measurements (Tan, 2004; Carmichael, 2003).

Due to the rapid economic development in Asia (especially in China), there is an increasing demand to maintain more accurate and updated emission inventories to improve modeling and understanding of the trends in emission variations. A new inventory of air pollutant emissions in Asia was developed in 2006 to support the Intercontinental Chemical Transport Experiment-Phase B (INTEX-B), which was funded by the National Aeronau-

* Corresponding author. E-mail: anxq@cams.cma.gov.cn

tics and Space Administration (NASA). The INTEX-B inventory improves and updates China's entire major anthropogenic inventory from the TRACE-P emission inventory because China's atmospheric emissions are known to have increased substantially during the past years following the dramatic growth of its economy and energy use (Zhang et al., 2007).

Since one of the major uncertainties in an air quality model is due to emissions inputs, which can have a significant influence on the simulation results (Russell and Dennis, 2000), a more accurate and up-to-date emission inventory is essential for improving air quality simulation. In an effort to quantify and evaluate the impact of emissions inputs on air quality simulation, the Community Multiscale Air Quality (CMAQ) modeling system (Byun and Schere, 2006) was used in this study driven by the NCAR/Penn State Mesoscale Model (MM5) meteorological fields. The air quality simulation results generated by the regional emission inventory of INTEX-B2006 (I06 EI) inputs were assessed in detail using observations from three regional atmospheric background stations of China. Although in addition to emission, there are many other factors influencing the model results such as dispersion, transportation and atmospheric transformations, in this article we focus on the impact of emission inventory on the model results.

The aim of this research is to evaluate the impact of the INTEX-B2006 (I06) emission inventory on SO_2, NO_x, CO and O_3 simulations in China to form some basis for modifying and improving emission inventories.

1 Methods and data

1.1 Emissions inventory data

To reflect the dramatic economic growth and energy use in Asia since 2001, especially in China, by implementing a series of improved methodologies and based on statistical data, the anthropogenic emissions from the regional emission inventory of INTEX-B2006 (Zhang et al., 2009) were updated from the TRACE-P inventory, which was prepared for the year 2000 and has received widespread application both within the TRACE-P mission and in subsequent Asian modeling studies (Streets et al., 2003a, 2003b). The INTEX-B2006 inventory includes the species SO_2, NO_x, CO, VOC, PM_{10}, $PM_{2.5}$, BC, and OC by sectors of power, industry, residential, and transportation and six VOC species by sector files. Only anthropogenic emissions are updated in the INTEX-B2006 inventory, and biomass burning emissions are still from the TRACE-P inventory (Streets et al., 2003a). The grid resolution of the emission inventory is $0.5° \times 0.5°$ and the SMOKE model was used to convert the emission inventory into the model format. The emission inventories of the key species of INTEX-B2006 are listed in **Table 1**.

The map of anthropogenic SO_2 and NO_x emissions in the INTEX-B2006 inventory (Zhang et al., 2009) shows that most emissions are distributed in the east of China, especially in the North China and the Yangtze River Delta regions. Therefore we mainly focus on these areas, including the three regional atmospheric background stations of Shangdianzi (SDZ) (representing North China), Linan (LN) (representing the Yangtze River Delta region) and Longfengshan (LFS) (representing the Northeast of China).

1.2 Observation data

The meteorological data of temperature, wind speed and wind direction from the three stations of Shangdianzi, Longfengshan and Linan were used to evaluate the model performance. All three stations are regional atmospheric background stations representing the atmospheric situations of North China, the Northeast of China and the Yangtze River delta (Meng et al., 2009). All measurement data quality was controlled according to standards (Lin et al., 2008; Meng et al., 2009; Xu et al., 2008). The SO_2, NO_x, CO and O_3 observations of the three stations were also compared with the model results to evaluate the inventory.

The Shangdianzi site (117.12°E, 40.65°N, 293.13 m a.s.l.) is located in the central area of North China about 120 km northeast of Beijing, and its topography and climate have the typical characteristics of the North China region. It was established by the China Meteorological Administration and selected as one of the earliest regional atmospheric background monitoring stations in 1981 (Lin et al., 2008). The LFS site (44.73°N, 127.60°E, 330.5 m a.s.l.) is located in a forest within Heilongjiang Province about 130 km northeast of Jilin and about 210 km northeast of Changchun. It is one of the four World Meteorological Organization Regional Background Stations in China (Meng et al., 2009). The LN site (30.18°E, 119.44°N, 139 m a.s.l.) is located in the Yangtze Delta region, about 50 km west of Hangzhou and about 210 km southwest of

Table 1 Anthropogenic emission of key species in China for the INTEX-B2006 inventory

Species	Power	Industry	Residential	Transportation	Total
SO_2 (Gg/year)	18333	9725	2838	123	31020
NO_x (Gg/year)	9197	5371	1166	5096	20830
CO (Gg/year)	2362	74936	55883	33709	166889
BC (Gg/year)	36	575	1002	198	1811
OC (Gg/year)	6	505	2606	101	3217
$PM_{2.5}$ (Gg/year)	1474	6932	4461	398	13266

Shanghai. It was also established and operated as one of the regional Global Atmospheric Monitoring stations in China by China Meteorological Administration (Xu, 2008).

1.3 Model introduction and setup

The Mesoscale Model of MM5v36 (Grell et al., 1994) was used to generate the meteorological fields (including wind, temperature, humidity, pressure, and other parameters) for the SMOKE and CMAQ. We selected some physical parameterization schemes in MM5, such as the MRF, Grell and cloud-cooling schemes for the boundary layer process, convective motion and radiation. The NCAR/NCEP reanalysis data, which were collected four times a day with a $1° \times 1°$ resolution, were used for the initial and boundary conditions in the MM5 model.

SMOKE was applied to convert the resolution of the emission inventory data of INTEX-B2006 to the resolution needed by an air quality model such as CMAQ. Emission inventories are available with an annual-total emissions value for each emission source. However, emissions data on an hourly basis, for each model grid cell and model layer as well as each model species, are typically required in air quality models. The SMOKE model transformed the emission inventory of INTEX-B2006 through temporal allocation, chemical speciation and spatial allocation, and generated the grid emissions to achieve the input requirements of the CMAQ model.

SMOKE can process various types of pollutants including criteria gaseous pollutants such as CO, NO*x*, VOC, NH_3, and SO_2; PM pollutants such as $PM_{2.5}$ and PM_{10}; as well as a large array of toxic pollutants, such as mercury, cadmium, benzene, and formaldehyde. Currently, several calculating schemes such as the plume rise calculation are used in SMOKE, and they can support point, area, mobile, and biogenic-source emissions processing modeling.

In this work, before the INTEX-B2006 inventory was put into SMOKE, much basic work had to be done. A lot of detailed information about the emission sources was set up for the emission inventory (EI) such as the Source Classification Code, Country, State and County Code, temporal spatial species profile, and cross references files based on some research results of different source characteristics in China and reference values of the Environmental Protection Agency (EPA). We rearranged the EI into inventory data analyzer format for the SMOKE model. **Figure 1** shows examples of temporal spatial profiles used in this work. After this preliminary work, the annual-total emissions of INTEX-B2006 were converted into hourly grid emissions data for CMAQ by SMOKE.

The CMAQ model, which includes different parts such as jproc, bcon, icon, cctm and mcip for the photolysis rate processor, the boundary condition processor, the initial condition processor, the chemical transport model and the meteorology data processor, was used in this work. Several gas-phase chemical mechanisms such as RADM, CB4 and SAPRC99 etc., linked to the aerosol module and aqueous chemistry, can be selected in CMAQ, and the CB4 scheme was used in this work.

The modeling domain was centered at 36.3°N, 103.8°E with a horizontal resolution of 36 km covering all of China with 140×116 grids for MM5 in this study (**Fig. 2**). To avoid boundary influences on the CMAQ results, the outer grids in MM5 domain were excluded and only 137×113 grids in CMAQ were used, with the same center. In the MM5 model, 27 layers with varying thicknesses were unequally distributed in the vertical dimension from the ground to a level of 100 hPa; 16 vertical layers extending from the surface to approximately 12 km were used in CMAQ, which were reduced from the 27 sigma levels of MM5 using mass-weighted averaging algorithms to reduce computational costs. The vertical layers in CMAQ were unevenly distributed and the surface layer was approximately 15 m. All the results that are presented here are for the lowest layer. For this evaluation, the year of 2006 was selected to simulate.

2 Results

2.1 Evaluation of the meteorological fields of MM5-CMAQ

Meteorological fields, especially wind speed and wind direction, are the major elements that influence the trans-

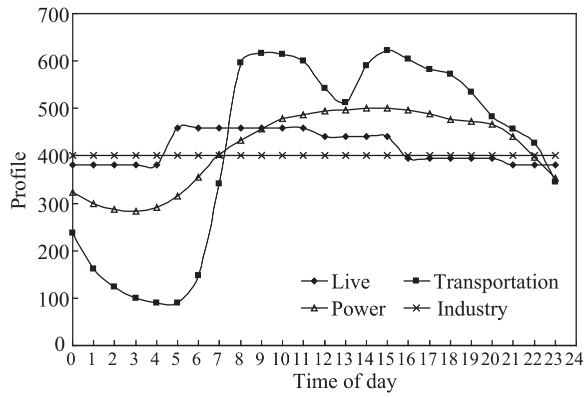

Fig. 1 Temporal spatial profiles for different sources.

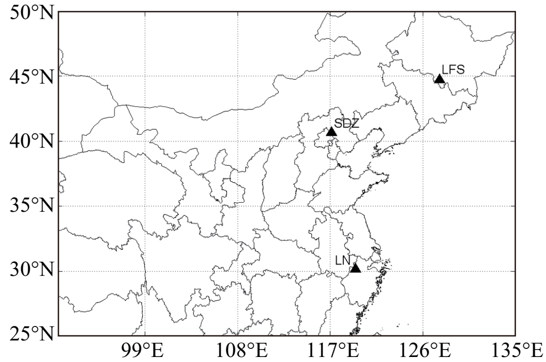

Fig. 2 Modeling domain and the location of SDZ, LFS and LN sites.

port, diffusion, interactions and deposition of air pollution. The accuracy of meteorological prediction is the most important factor related to air quality model performance. The main factors such as wind speed, wind direction and temperature etc., which related closely with pollution diffusion, are analyzed in this article.

Comparisons between the observed and simulated daily mean temperature at the three stations (Figure omitted) showed that the temperature feature could be simulated by the model and the simulation curve was nearly a repeat of the observation. Moreover, the model was able to produce the major features of the observed fields of wind speed and wind direction (Figure omitted), and correlation coefficients (R) for the three species were high, especially for temperature, with R exceeding 0.99 at the three stations (**Fig. 3**). The qualitative statistics summaries of the calculated meteorological fields at SDZ, LFS and LN are presented in **Table 2**. The mean simulated temperature was slightly less than the mean observed and the mean biases of SDZ, LFS and LN were –0.72, –0.76 and –0.81°C, respectively. The root mean square errors (RMSE) for temperature in the three stations were small and less than 2.0°C. The differences between mean simulated and observed wind speed in SDZ, LFS and LN were not too great and RMSE were less than 1.0 m/sec. For wind direction, LFS had the lowest RMSE and the highest index of agreement (IA), and had a better simulation, with SDZ and LN next.

In all, the statistical analyses show that the current system has good performance with small and reasonable standard deviations and high correlations. The IA statistics are the same as R and show the IA between the simulated and the observed. The IA values for temperature, wind speed and direction in the three stations are high and demonstrate a good consistency between simulations and observations.

In order to display the model performance for the meteorological fields in different months, R at the three stations are presented in **Fig. 4**. It can be seen that the simulations of temperature, wind speed and wind direction for each month at LFS were very good and almost all R values exceeded 0.8. For temperature, all correlation

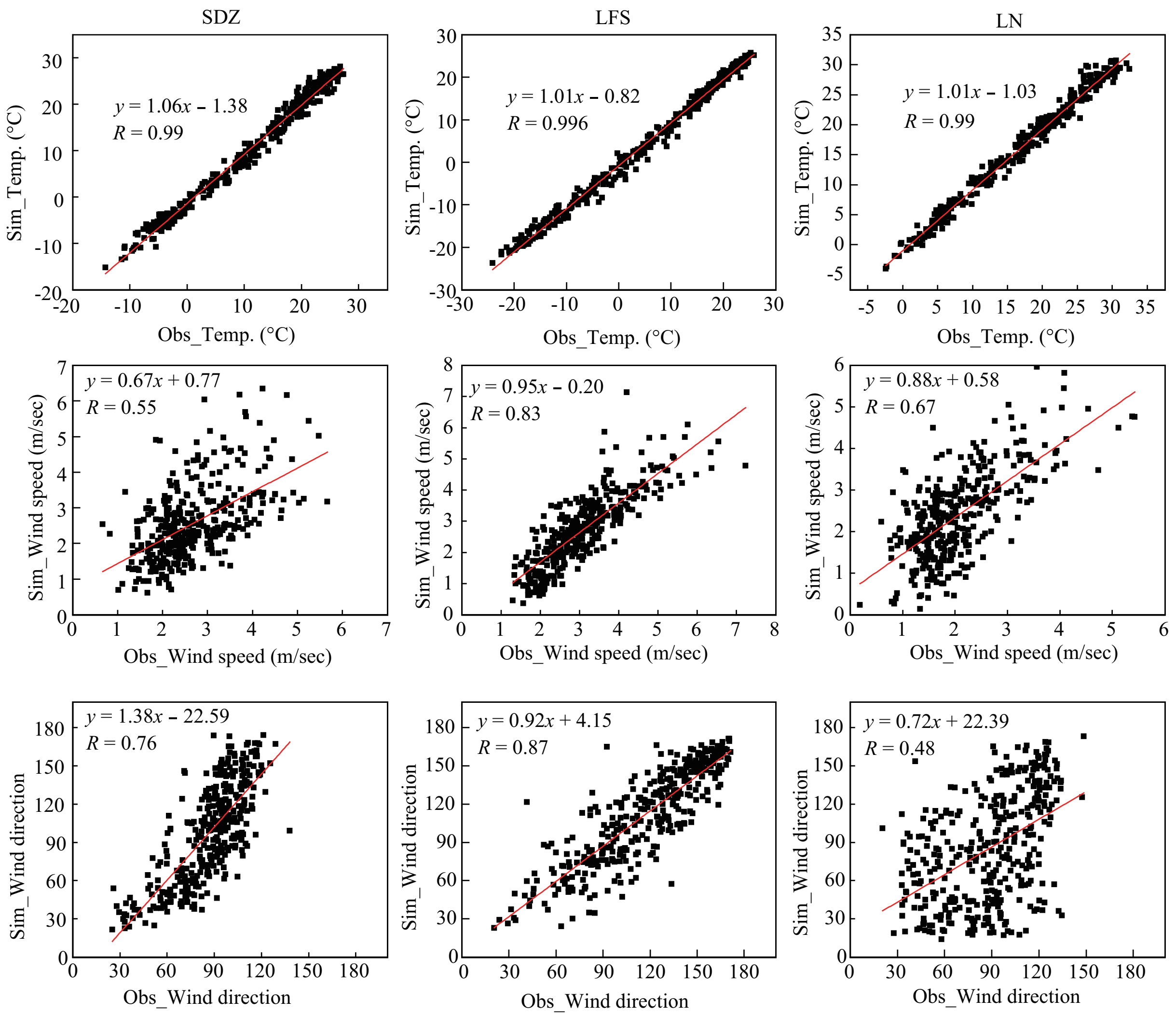

Fig. 3 Correlation coefficients between observed (Obs) and simulated (Sim) temperature, wind speed and wind direction at SDZ, LFS and LN.

Table 2 Statistical summaries of the meteorological comparisons of the model results with observation results of the three regional atmospheric background stations in China

	Temperature (°C)			Wind speed (m/sec)			Wind direction (°)		
Statistics	SDZ	LFS	LN	SDZ	LFS	LN	SDZ	LFS	LA
Mean_Obs	10.65	5.05	16.90	2.67	3.08	2.03	87.11	117.27	87.83
Mean_Sim	9.93	4.29	16.10	2.55	2.71	2.37	98.02	112.09	84.82
MB	–0.72	–0.76	–0.81	–0.11	–0.37	0.34	10.91	–5.18	–3.01
RMSE	1.81	1.54	1.37	0.93	0.73	0.85	28.08	19.51	38.09
IA	0.99	0.996	0.99	0.73	0.88	0.78	0.76	0.92	0.67

Mean_Obs: mean observed; Mean_sim: mean simulated;

MB: mean bias, $\text{MB} = \frac{1}{N}\sum_{i=1}^{N}(P_i - O_i)$

RMSE: root mean square error, $\text{RMSE} = \left[\frac{1}{N}\sum_{i=1}^{N}(P_i - O_i)^2\right]^{1/2}$

IA: index of agreement, $\text{IA} = 1 - \sum_{i=1}^{N}\left(P_i - O_i)^2\right) / \sum_{i=1}^{N}\left(|P_i - \bar{O}| + |O_i - \bar{O}|\right)^2$

(Bounded between 0 and 1, where IA = 1 is a perfect model).

coefficients were higher than 0.8 except in July at SDZ and LN. Wind speed at SDZ had lower R in summertime, and R values for the other two stations were higher except in October at LN. Compared to SDZ and LFS, wind direction at LN had lower R (less than 0.5) in January, September and October.

2.2 Evaluating emissions by comparing model simulations with observations

2.2.1 Daily simulations

The time series of simulated SO_2, NOx, CO and O_3 daily mean concentrations based on INTEX-B2006 EI were compared with the observations at the three stations of SDZ, LFS and LN (Figure omitted). In general, the model was able to capture the overall features and variability of observations. The simulated daily SO_2, NOx and O_3 variances accorded well with the observations, and the SO_2 simulations for SDZ and LFS slightly exceeded the observations during summertime. Although the model could produce the daily trend of CO, there was significant underestimation of the observations at the three stations,

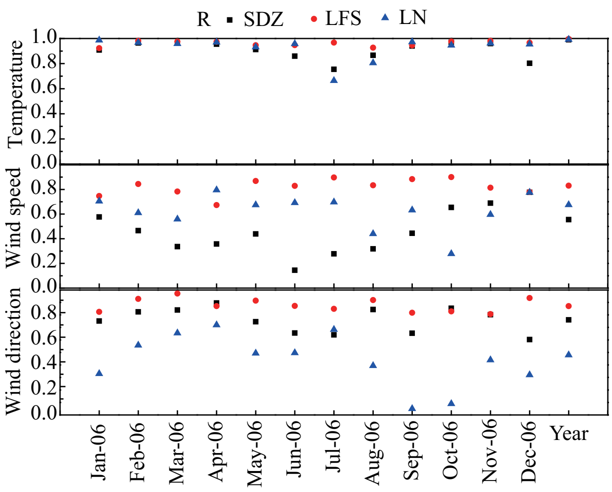

Fig. 4 Correlation coefficients between observed and simulated temperature, wind speed and wind direction at SDZ, LFS and LN by month.

by factors of about two-third or one-half. In previous publications (Streets et al., 2003a, 2003b), the uncertainty of CO emission in Asia was estimated to be ±185%. The high uncertainty in CO emission results in underestimation of CO.

Figure 5 shows correlation coefficients (R) of SO_2, NOx CO and O_3 at the three stations. In general, there were good coefficients for the four species, especially for SO_2 and NOx, which were higher than 0.6. Although the simulated CO concentrations were considerably underestimated, the correlation coefficients were higher than 0.56 for CO, indicating that model could capture the daily variance character of CO.

2.2.2 Monthly simulations

The comparisons of simulated and observed monthly mean values of the four species at the three stations are presented in **Fig. 6**. It can be seen that the simulated monthly variances of NOx and O_3 agree with the observed values at SDZ station; but NOx and CO simulations at SDZ were under-predicted, especially for CO, by about one-third of the observations. SDZ site is likely close to local emission sources from the Beijing area; and the 0.5 × 0.5 grid resolution of the INTEX-B2006 EI used in this study is not capable of accounting for the impacts of strong regional sources on stations. At the two stations LFS and LN, the model could capture the characteristics of monthly variance trends of SO_2, NOx, O_3 and CO, although the simulated CO monthly mean values were about one half of the observed values.

The correlation coefficients for each month at the three stations are presented in **Fig. 7** to aid the detailed comparison of model performance for the four species in different months. For SO_2, SDZ had poor R during summertime, especially in July and August. We can see (**Fig. 4**) that the wind speed and wind direction simulations for SDZ in summertime were not as good as in other months, especially for wind speed, with lower R value in June, July and August. Thus the bad SO_2 simulations at

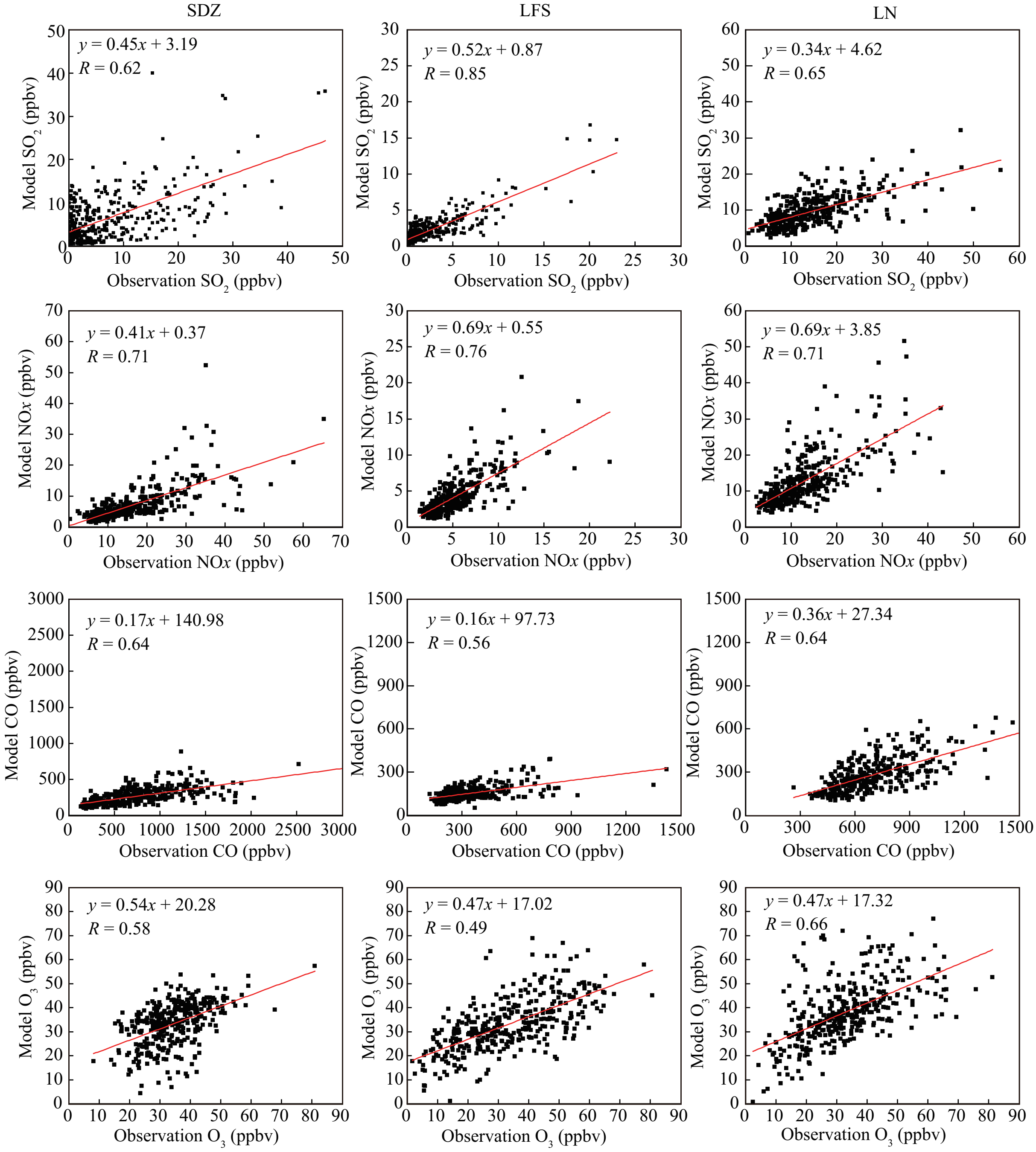

Fig. 5 Correlation coefficients between observed and simulated daily SO_2, NOx, CO and O_3 at SDZ, LFS and LN.

the SDZ site during summertime are partly related with the model's poor depiction of the wind field compared to other months. The model was able to capture the SO_2 monthly trend of the LFS site very well (**Fig. 6**) and the correlation coefficients of SO_2 at the LFS site are higher than 0.4 for all months. Moreover, we can find that the model had higher performance in simulating wind speed and direction at the LFS site (**Fig. 4**). LN had almost the same SO_2 monthly trend between simulated and observed values, but low R value in August, September and October, related with poor simulation of wind direction in these three months (**Fig. 4**). Furthermore, October had the lowest R, related with both poor wind speed and direction. Generally, the simulated SO_2 monthly values were slightly lower than the observations except at the SDZ and LFS site during summertime, indicating that the simulated emissions were slightly low except for summer at SDZ and LFS.

For NOx simulations at the SDZ site, as with SO_2, summertime exhibited R values less than 0.5. In addition, the simulations were slightly lower than the observations for each month at the SDZ site. There were no notable differences between the monthly mean NOx simulations

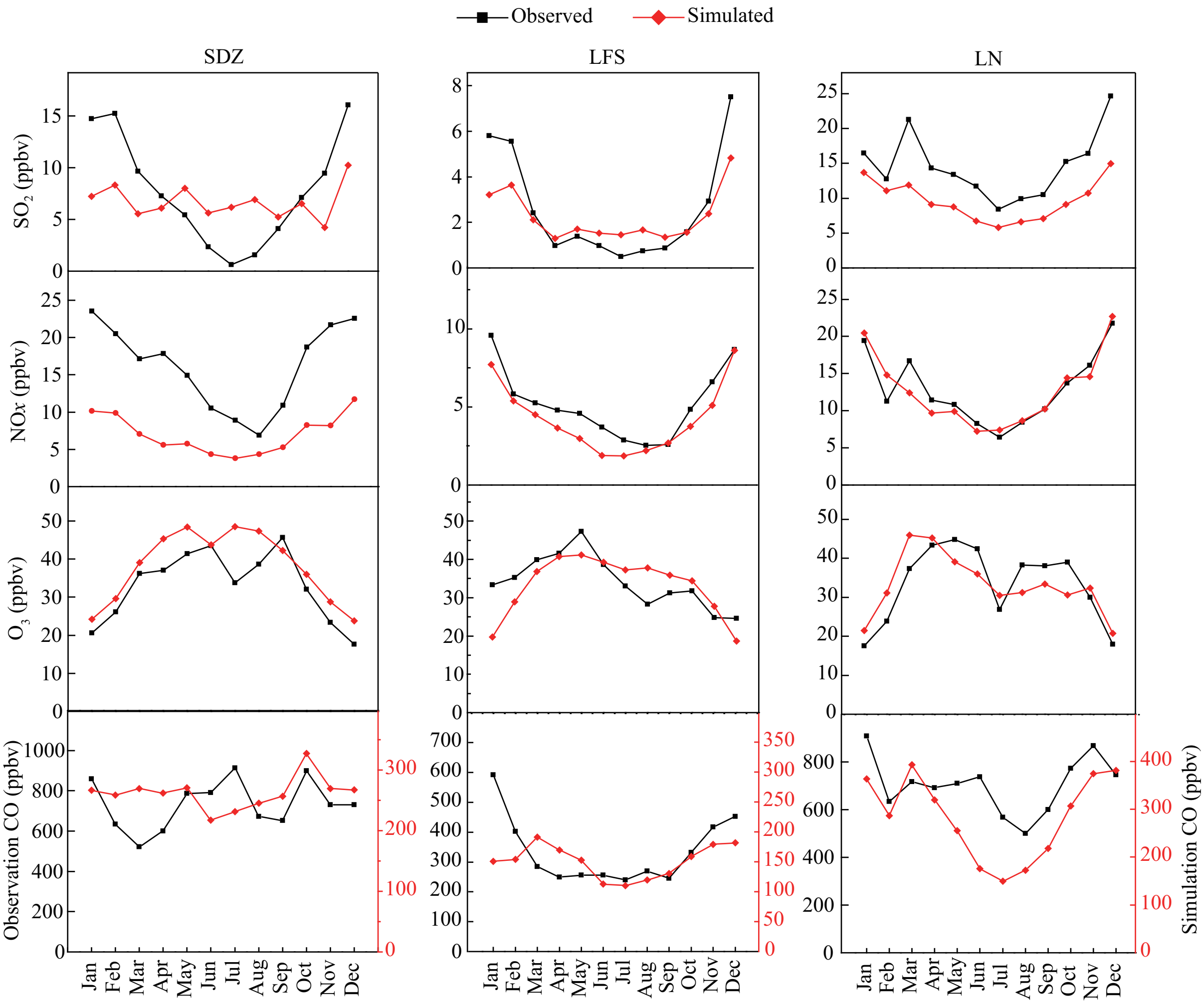

Fig. 6 Observed and simulated monthly mean values of SO_2, NOx, CO and O_3 at the sites SDZ, LFS and LN.

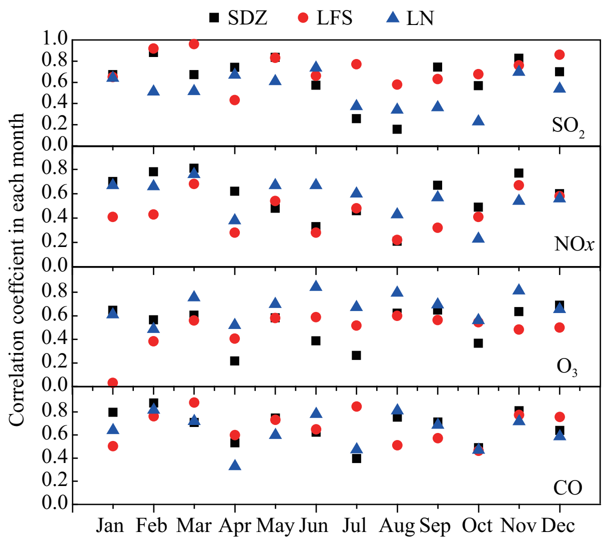

Fig. 7 Correlation coefficients between observed and simulated SO_2, NOx, CO and O_3 at SDZ, LFS and LN by month.

and observations for LFS, but the R values for each month at the LFS site were not consistently high as obtained for SO_2. Several months such as April, June and August exhibited slightly lower R, indicating that some factors influence NOx simulations different from SO_2. The model was able to capture the NOx monthly trend of the LN site very well (**Fig. 6**), and the monthly mean simulations and observations were almost the same in some months. The correlation coefficients for NOx at the LN site for each month were higher except in October, related to the poor performance in terms of wind speed and direction.

For O_3, the simulated monthly trend was almost consistent with the observed at the three sites and the differences between the monthly mean simulation and observation values were slight (**Fig. 6**). Compared to SDZ and LFS, LN had higher R for each month, but R for SDZ was lower in April and July, and LFS had the lowest R value in January, indicating that some complicated factors influenced the model performance for O_3.

Although CO concentrations at the three stations were grossly underestimated, the correlation coefficients for each month were consistently higher. This shows that the CO emission inventory is very much underestimated, although the model could capture the CO variance characteristics well.

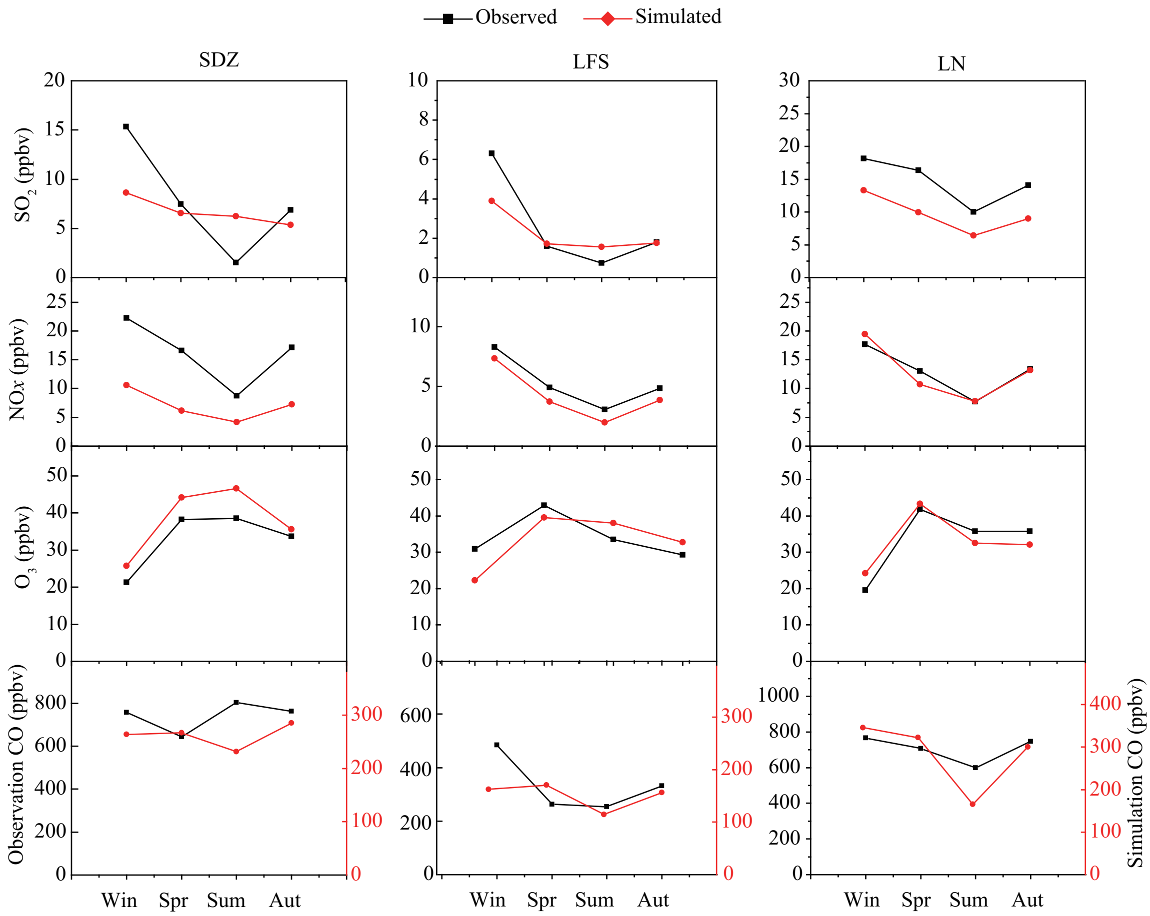

Fig. 8 Observed and simulated seasonal mean values of SO_2, NO*x*, CO and O_3 at the stations SDZ, LFS and LN.

2.2.3 Seasonal simulations

In order to discuss the model performance in capturing the seasonal characteristics of observations, comparisons between the observed and simulated seasonal mean values of SO_2, NO*x*, CO and O_3 at the stations of SDZ, LFS and LN are shown in **Fig. 8**. It can be seen that the simulated seasonal mean values of SO_2, NO*x* and O_3 are closely in accordance with the observed values at the three stations, except for SO_2 at SDZ in summer. The seasonally averaged CO simulations at the three stations were also underestimated by about two-third at SDZ, and one half at LFS and LN.

Correlation coefficients in different seasons are plotted in **Fig. 9**. For SO_2, the correlation coefficients were all higher than 0.5 except at SDZ in summer. NO*x* showed a more complicated seasonal character compared to SO_2, and SDZ had poor *R* in summer and spring, and LFS in winter and spring. However, CO simulations were grossly underestimated. The model can capture seasonal trends, with *R* values all higher than 0.4. O_3 showed the same behavior as SO_2. Compared to the other seasons, summer had the lowest *R* values for SO_2 and O_3. Thus in view of *R* values, SO_2 and O_3 were not well predicted in summer, which is partly related to poor simulations of temperature and wind.

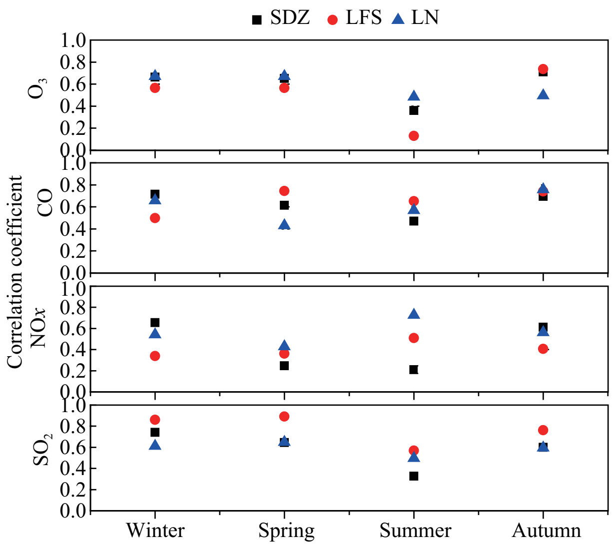

Fig. 9 Correlation coefficients between observed and simulated SO_2, NO*x*, CO and O_3 at SDZ, LFS and LN for spring, summer, autumn and winter.

2.2.4 Diurnal simulations

Figure 10 shows the comparison between the observed and simulated mean diurnal variances of SO_2, NO*x*, O_3 and CO at the three stations. The differences between the simulated and observed SO_2 curves at SDZ and LFS are significant, and the observed diurnal peak at about 14:00 was not simulated by the model. For NO*x* at SDZ, the daily simulation variance curve basically agreed with observation, but the simulated value was about one-half of observation. The daily NO*x* change at LFS was not significant. Diurnal SO_2 and NO*x* changes at LN station were basically captured by the model except that the simulated SO_2 value was slightly less than observation. Compared to SO_2 and NO*x*, the diurnal ozone change characteristics were perfectly depicted by the model, and O_3 values reached their peak at about 14:00 and dropped to the lowest level at 06:00. The simulated curves of O_3 were accordance with the observed, especially at LFS and LN. Although simulated values remained less than observations, diurnal CO variance trends were basically simulated by the model. In all, daily variances of the four species at LN were simulated well. Compared to SO_2, NO*x* and CO, O_3 showed a different diurnal change.

3 Discussion and summary

Emission inventory is a key factor that influences air quality model simulation, and also plays an important role in managing pollution. The newest and most popular emission inventory of INTEX-B2006 has been used and evaluated, based on simulation results from the CMAQ model compared with observations from three regional atmospheric background stations of China. The statistical analysis shows that the model results with INTEX-B2006 EI can basically capture the temporal characteristics of the three sites observations.

However, for some special periods such as summertime, the model did not exhibit the same level of performance as for the other seasons, which is partly related to poor simulations of meteorological factors such as wind. Compared to the species of SO_2, NO*x* and O_3, CO simulations were grossly underestimated by about two-third in SDZ and one-half in LFS and LN, arising from high uncertainty in INTEX-B2006 CO emission (Streets et al., 2003a, 2003b).

The selected regional atmospheric background stations represent the different three important regions of China.

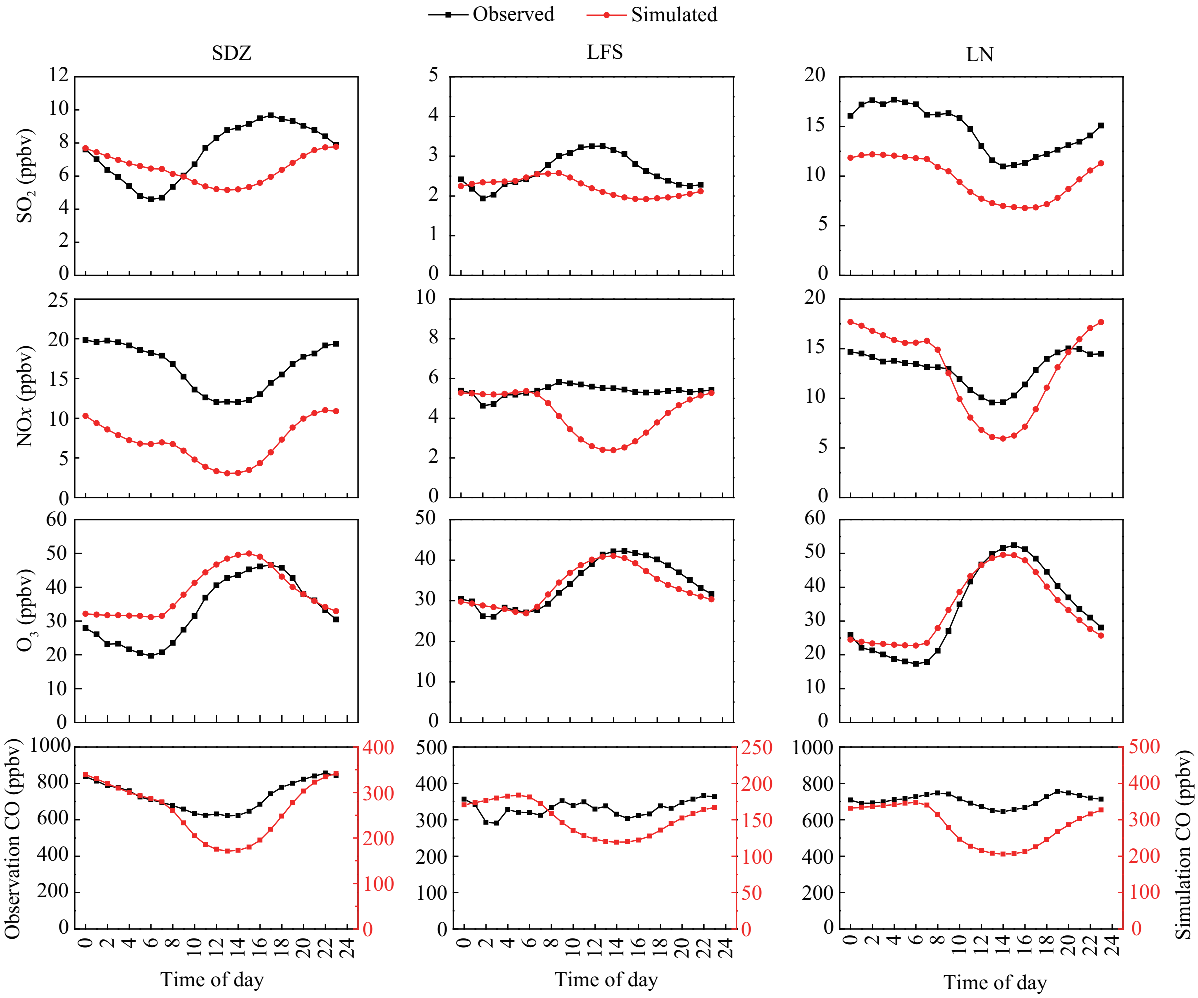

Fig. 10 Observed and simulated mean diurnal variation of SO_2, NO*x*, CO and O_3 at the stations SDZ, LFS and LN.

Among the three stations, LFS showed good simulations for meteorological factors such as temperature, wind speed and wind direction, as well as SO_2 and NOx simulations. Compared to the other two sites, SDZ showed poor simulations for SO_2, especially in summertime, related to poor meteorological simulation of parameters such as wind speed in this period. The simulated CO was underestimated greatly at the SDZ station, by about two-third of the observed values. The reasons include the uncertainty in CO emission data and close location to the Beijing and Tianjin area, as well as the inability of the regional emission inventory of INTEX-B2006 to depict the characteristics of strong local sources. Therefore the improvement and updating of the current emission inventory is an urgent task to enable good air quality simulation and gain a thorough understanding of pollution.

Acknowledgments

This work was supported by the Chinese Ministry of Science and Technology (No. 2011CB403404), the CAMS Basic Research Funds-regular (No. 2010Y005), the Specific Team Fund of CAMS (No. 2010Z002) and the National Natural Science Foundation of China (No. 40875086).

References

Bergin M S, Noblet G S, Petrini K, Dhieux J R, Milford J B, Harley R A,1999. Formal uncertainty analysis of a Lagrangian photochemical air pollution model. *Environmental Science and Technology*, 33(7): 1116–1126.

Bond T C, Streets D G, Yaber K F, Nelson S M, Woo J H, Klimont Z, 2004. A technology-based global inventory of black and organic carbon emissions from combustion. *Journal of Geophysical Research*, 109: D14203.

Byun D, Schere K L, 2006. Review of the governing equations, computational algorithms, and other components of the Models-3 Community Multiscale Air Quality (CMAQ) modeling system. *Applied Mechanics Reviews*, 59(2): 51–77.

Cao G L, Zhang X Y, Zheng F C, 2006. Inventory of black carbon and organic carbon emissions from China. *Atmospheric Environment*, 40(34): 6516–6527.

Carmichael G R, Tang Y, Kurata G, Uno I, Streets D G, Thongboonchoo N et al., 2003. Evaluating regional emission estimates using the TRACE-P observations. *Journal of Geophysical Research*, 108(D21): 8810. DOI: 10.1029/2002JD003116.

Grell G A, Dudhia J, Stauffer D R A, 1994. A description of the Fifth Generation Penn 15 State/NCAR Mesoscale Model (MM5), NCAR Technical Note, 1994, NCAR/TU-398+STR, 138.

Hanna S R, Chang J C, Fernau M E, 1998. Monte Carlo estimates of uncertainties in a predictions by photochemical grid model (UAM-IV) due to uncertainties in input variables. *Atmospheric Environment*, 32(21): 3619–3628.

Jacob D J, Crawford J, Kleb M M, Connors V S, Bendura R J, Raper J L et al., 2003. Transport and chemical evolution over the Pacific (TRACE-P) mission: Design, execution, and first results. *Journal of Geophysical Research*, 108(D20): 8781. DOI: 10.1029/2002JD003276.

Jiang X K, Tang X Y, 2002. Research on Air Pollution Control Strategies for Beijing. Beijing EPA, Peking University. 1–268.

Lin W, Xu X, Zhang X, Tang J, 2008. Contributions of pollutants from North China Plain to surface ozone at the Shangdianzi GAW Station. *Atmospheric Chemistry and Physics*, 8(19): 5889–5898.

Meng Z Y, Xu X B, Yan P, Ding G A, Tang J, Lin W L et al., 2009. Characteristics of trace gaseous pollutants at a regional background station in Northern China. *Atmospheric Chemistry and Physics*, 9(3): 927–936.

Placet M, Mann C O, Gilbert R O, Niefer M J, 2000. Emissions of ozone precursors from stationary sources: a critical review. *Atmospheric Environment*, 34(12-14): 2183–2204.

Russell A, Dennis R, 2000. NARSTO critical review of photochemical models and modeling. *Atmospheric Environment*, 34(12-14): 2283–2324.

Streets D G, Bond T C, Carmichael G R, Fernandes S D, Fu Q, He D et al., 2003a. An inventory of gaseous and primary aerosol emissions in Asia in the year 2000. *Journal of Geophysical Research*, 108(D21): 8809. DOI: 10.1029/2002JD003093.

Streets D G, Gupta S, Waldhoff S T, Wang M Q, Bond T C, Bo Y, 2001. Black carbon emissions in China. *Atmospheric Environment*, 35(25): 4281–4296.

Streets D G, Yarber K F, Woo J H, Carmichael G R, 2003b. Biomass burning in Asia: annual and seasonal estimates and atmospheric emissions. *Global Biogeochemical Cycles*, 17(4):1099. DOI: 10.1029/2003GB002040.

Tan Q, Chameides W L, Streets D G, Wang T, Xu J, Bergin M et al., 2004. An evaluation of TRACE-P emission inventories from China using a regional model and chemical measurements. *Journal of Geophysical Research*, 109(D22): D22305. DOI: 10.1029P2004JD005071.

Xu X, Lin W, Wang T, Yan P, Tang J, Meng Z et al., 2008. Long-term trend of surface ozone at a regional background station in eastern China 1991–2006: enhanced variability. *Atmospheric Chemistry and Physics*, 8(10): 2595–2607.

Zhang Q, Streets D G, Carmichael G R, He K B, Huo H, Kannari A et al., 2009. Asian emissions in 2006 for the NASA INTEX-B mission. *Atmospheric Chemistry and Physics*, 9(14): 5131–5153.

Zhang Q, Streets D G, He K B, Klimont Z, 2007. Major components of China's anthropogenic primary particulate emissions. *Environmental Research Letters*, 2(4): 45027. DOI: 10.1088/1748-9326/2/4/045027.

JOURNAL OF ENVIRONMENTAL SCIENCES

(http://www.jesc.ac.cn)

Aims and scope

Journal of Environmental Sciences is an international academic journal supervised by Research Center for Eco-Environmental Sciences, Chinese Academy of Sciences. The journal publishes original, peer-reviewed innovative research and valuable findings in environmental sciences. The types of articles published are research article, critical review, rapid communications, and special issues.

The scope of the journal embraces the treatment processes for natural groundwater, municipal, agricultural and industrial water and wastewaters; physical and chemical methods for limitation of pollutants emission into the atmospheric environment; chemical and biological and phytoremediation of contaminated soil; fate and transport of pollutants in environments; toxicological effects of terrorist chemical release on the natural environment and human health; development of environmental catalysts and materials.

For subscription to electronic edition

Elsevier is responsible for subscription of the journal. Please subscribe to the journal via http://www.elsevier.com/locate/jes.

For subscription to print edition

China: Please contact the customer service, Science Press, 16 Donghuangchenggen North Street, Beijing 100717, China. Tel: +86-10-64017032; E-mail: journal@mail.sciencep.com, or the local post office throughout China (domestic postcode: 2-580).

Outside China: Please order the journal from the Elsevier Customer Service Department at the Regional Sales Office nearest you.

Submission declaration

Submission of an article implies that the work described has not been published previously (except in the form of an abstract or as part of a published lecture or academic thesis), that it is not under consideration for publication elsewhere. The submission should be approved by all authors and tacitly or explicitly by the responsible authorities where the work was carried out. If the manuscript accepted, it will not be published elsewhere in the same form, in English or in any other language, including electronically without the written consent of the copyright-holder.

Submission declaration

Submission of the work described has not been published previously (except in the form of an abstract or as part of a published lecture or academic thesis), that it is not under consideration for publication elsewhere. The publication should be approved by all authors and tacitly or explicitly by the responsible authorities where the work was carried out. If the manuscript accepted, it will not be published elsewhere in the same form, in English or in any other language, including electronically without the written consent of the copyright-holder.

Editorial

Authors should submit manuscript online at http://www.jesc.ac.cn. In case of queries, please contact editorial office, Tel: +86-10-62920553, E-mail: jesc@263.net, jesc@rcees.ac.cn. Instruction to authors is available at http://www.jesc.ac.cn.

Journal of Environmental Sciences (Established in 1989)
Vol. 25 No. 3 2013

Supervised by	Chinese Academy of Sciences	**Published by**	Science Press, Beijing, China
Sponsored by	Research Center for Eco-Environmental		Elsevier Limited, The Netherlands
	Sciences, Chinese Academy of Sciences	**Distributed by**	
Edited by	Editorial Office of Journal of	Domestic	Science Press, 16 Donghuangchenggen
	Environmental Sciences		North Street, Beijing 100717, China
	P. O. Box 2871, Beijing 100085, China		Local Post Offices through China
	Tel: 86-10-62920553; http://www.jesc.ac.cn	Foreign	Elsevier Limited
	E-mail: jesc@263.net, jesc@rcees.ac.cn		http://www.elsevier.com/locate/jes
Editor-in-chief	Hongxiao Tang	**Printed by**	Beijing Beilin Printing House, 100083, China

CN 11-2629/X **Domestic postcode: 2-580** **Domestic price per issue RMB ¥ 110.00**

ISSN 1001-0742